 Proceedings of ICCES'08, pp.651-670

Analysis of Flexible Media Transport Characteristics of Crown Roller and Its Application to Design

Iizuka Yoichiro[1], Hiroshi Yamaura

Summary

Crown rollers are often used in the flexible media transport mechanism consists of a rubber layered roller and a steel roller. In this paper, the flexible media transport characteristics of crown roller is investigated theoretically. The purpose of this study is to analyze the flexible media transport characteristics such as longitudinal distribution of nip pressure, traction and transport velocity and so on, and to develop the design method of crown roller that has desired characteristics.

In the first step of this study, a numerical analysis method of the slip and traction characteristics between a rubber-layered roller and a mated steel roller based on the Boundary-Element Method was established. Under the assumption of a plane-strain, Green's functions of a rubber roller with a rigid core based on polar coordinates were analytically derived in our method. A contact problem of two rollers under normal and tangential loading forces was numerically analyzed using derived Green's function. Coulomb's friction law, with a constant coefficient of friction, and no difference between the adhesion and the sliding coefficient of friction, was considered in the contact problem. The normal and tangential contact pressures, strain of rubber surface, nip width and indentation depth were iteratively calculated so as to satisfy the given normal and tangential loading forces. The tangential velocity ratio between the two rollers was also calculated for various parameter values. It was confirmed that the numerical results agree well with the experimental ones.

In the second step of this study, an analytical approach that can estimate flexible media transfer characteristics of crown rollers was developed. In the analysis, two types of crown rollers, i.e. a rubber roller with crown shape in its internal diameter and a steel roller with crown shape in its diameter, were examined. And based on analysis results, a design approach of crown shape which can realize uniform longitudinal distribution of nip pressure was proposed. Designed crown rollers were fabricated and the performances of them were confirmed with experiment.

Introduction

For the flexible media transport mechanism composed of long rollers, it is very important to uniform longitudinal distribution of the nip pressure, traction, transport velocity, and so on. The deviation of longitudinal distribution of nip pressure is mainly subjected to the deflection of the roller shaft. Lots of methods that can

[1]Department of Mechanical and Control Engineering, Tokyo Institute of Technology. e-mail: iizuka.y.ab@m.titech.ac.jp

reduce the deviation have been developed and used practically. One of the methods involves a technique to change the diameter of the roller along the longitudinal axis, namely crown roller or crowning roller. Dimensions of the crown roller are designed experientially, because theoretical design method has not been revealed yet. Purpose of this study is to develop the analytical method of flexible media transport characteristics of crown roller and establish the theoretical design method of the crown roller.

Some researchers have been focused on a contact problem in a flexible media feeding mechanism. Soong and Li[8] considered a sheet in the nip of two cylinders and calculated pressure distribution for a normal load. In order to obtain traction characteristics of a feeding mechanism analytically, normal and tangential load should be considered. Soong and Li[9] proposed an analytical technique to calculate the traction characteristic between a rubber-layered roller and paper. They assumed a general stress function by the Fourier series in polar coordinates. In a nominal contact problem, their collocation method calculates the normal and tangential pressures at a contact area, tangential velocity ratios of two rollers and paper. Kalker[10] proposed a numerical algorithm to solve a rolling contact problem of viscoelastic multilayered cylinders with dry friction based on Bentall and Johnson[5]. Recently, this problem is focused upon and discussed in a research working group of the Japan Society for Precision Engineering. Wu et al. [11] investigated the traction characteristics of a paper and rollers experimentally. Okamoto et al.[12] analyzed the same problem by using a commercial FEM software and investigated the effects of friction, non-linearity of elastic modulus and large deformation, stress relaxation, rotating speed and the edge effect of a short roller as well as a normal and tangential load, and showed the validity and usefulness of the numerical analysis by experiment for short rollers. However, considering the fact that the actual feeding rollers in printers and copiers are longer than 200mm, it is almost impossible to numerically analyze the effect of a non-uniform nip load and skewed angle of such long feeding rollers by FEM.

Accordingly, in the first step of this paper a numerical analysis of the slip and traction characteristics between a rubber-layered roller and a mated rigid roller based on the Boundary-Element Method is presented. In order to investigate the basic contact characteristics of a rubber roller, the situation of no flexible madia between the two rollers is considered. The Green's function of a rubber-layered roller based on polar coordinates is obtained under the plane-strain condition, and then by using this Green's function, the relation of load force and penetration depth of the two rollers is calculated. The validity of the calculated results are shown by the experimental results.

In the second step, the crown roller is investigated based on the results of the

first step. Long rollers whose shaft deflection cannot be ignored have the longitudinal distribution of the nip pressure. In this case, the rubber deformation is three-dimentional but it can be modeled with two-dimensional contact mentioned before because the out-of-plane strain is much smaller than the plane strain. Thus, an analytical method that is based on the results of the two-dimensional contact analysis and can estimate the longitudinal distribution of nip pressure of the long rollers is developed. The analytical method is applied to a design method of the crown shape that can realize uniform longitudinal distribution of nip pressure. Two types of crown rollers i.e. a rubber roller with crown shape in its internal diameter and a steel roller with crown shape in its diameterare, defined and design procedures of these rollers are shown. Dsigned crown rollers are fabricated and the performances of them are confirmed with experiment.

Green's Function Derivation

Basic Equation and General Solution

Figure 1 depicts an analytical model of a rubber-layered steel roller and a mated steel roller. The rubber is deformed by contact with the mated steel roller. Because Young's modulus of steel is larger than 10^5 times of that of rubber, the deformation of steel parts is ignored. Uniform contact along the axial direction of the rollers is assumed in this analysis and only the deformation of rubber in a section is considered under the assumption of the plane-strain.

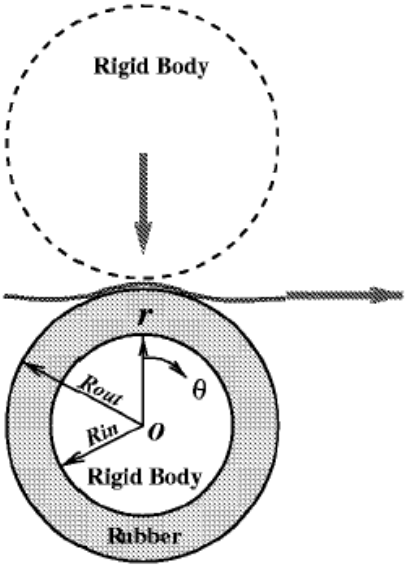

Figure 1: Analitical model of a rubber roller

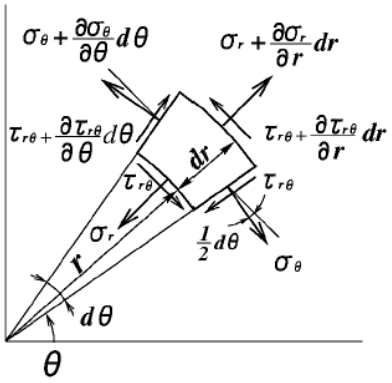

Figure 2: Infinitely small element and stress

Figure 2 shows an infinitely small element and definition of stress. The equilibrium equations of stress are given by

$$\frac{\partial \sigma_r}{\partial r} + \frac{1}{r}\frac{\partial \tau_{r\theta}}{\partial \theta} + \frac{\sigma_r - \sigma_\theta}{r} = 0 \quad (1)$$

$$2\frac{\tau_{r\theta}}{r} + \frac{\partial \tau_{r\theta}}{\partial r} + \frac{1}{r}\frac{\partial \sigma_\theta}{\partial \theta} = 0 \quad (2)$$

By substituting Hooke's Law into stress σ_r and $\tau_{r\theta}$, these equations are represented by normal and tangential deformation u, v.

$$\kappa\left\{\frac{\partial^2 u}{\partial r^2} + \frac{1}{r}\frac{\partial u}{\partial r} - \frac{u}{r^2}\right\} + \frac{\beta}{r}\frac{\partial^2 v}{\partial r \partial \theta} - \left\{\frac{\kappa^2-\beta^2}{2(1+\nu)} + \kappa\right\}\frac{1}{r^2}\frac{\partial v}{\partial \theta} + \frac{\kappa^2-\beta^2}{2(1+\nu)}\left\{\frac{1}{r}\frac{\partial^2 v}{\partial \theta \partial r} + \frac{1}{r^2}\frac{\partial^2 u}{\partial \theta^2}\right\} = 0 \quad (3)$$

$$\frac{\beta}{r}\frac{\partial^2 u}{\partial \theta \partial r} + \frac{\kappa}{r^2}\left\{\frac{\partial u}{\partial \theta} + \frac{\partial^2 v}{\partial \theta^2}\right\} + \frac{\kappa^2-\beta^2}{2(1+\nu)}\left\{\frac{1}{r^2}\frac{\partial u}{\partial \theta} + \frac{1}{r}\frac{\partial v}{\partial r} - \frac{v}{r^2} + \frac{1}{r}\frac{\partial^2 u}{\partial r \partial \theta} + \frac{\partial^2 v}{\partial r^2}\right\} = 0, \quad (4)$$

where E and ν are a Young's modulus and Poisson's ratio of rubber, respectively. Notation κ and β are constants related to ν as follows: $\kappa = 1-\nu^2$, $\beta = \nu(1+\nu)$.

In order to solve these partial differential equations, Eqs.(3) and (4), u and v as two Fourier series are defined as followings,

$$u \equiv G_0(r) + \sum_{k=1}^{\infty} G_{ck}(r)\cos k\theta + \sum_{k=1}^{\infty} G_{sk}(r)\sin k\theta \quad (5)$$

$$v \equiv K_0(r) + \sum_{k=1}^{\infty} K_{ck}(r)\cos k\theta + \sum_{k=1}^{\infty} K_{sk}(r)\sin k\theta \quad (6)$$

Notation k represents number of harmonics. After substituting Eqs.(5) and (6) into Eqs.(3) and (4), an independent variable r is transformed into a new variable t with $r = e^t$ in order to obtain six ordinary differential equations related with

$G_0(t), K_0(t), G_{ck}(t), G_{sk}(t), K_{ck}(t), K_{sk}(t)$.

$$\left(\frac{d^2}{dt^2}-1\right)G_0=0, \quad \left(\frac{d^2}{dt^2}-1\right)K_0=0 \tag{7}$$

$$\left.\begin{aligned}
&\left\{\kappa\frac{d^2}{dt^2}-(\kappa+\alpha k^2)\right\}G_{ck}+\left\{(\beta+\alpha)\frac{d}{dt}-(\kappa+\alpha)\right\}kK_{sk}=0\\
&\left\{\kappa\frac{d^2}{dt^2}-(\kappa+\alpha k^2)\right\}G_{sk}-\left\{(\beta+\alpha)\frac{d}{dt}-(\kappa+\alpha)\right\}kK_{ck}=0\\
&\left\{\alpha\frac{d^2}{dt^2}-(\kappa k^2+\alpha)\right\}K_{ck}+\left\{(\beta+\alpha)\frac{d}{dt}+(\kappa+\alpha)\right\}kG_{sk}=0\\
&\left\{\alpha\frac{d^2}{dt^2}-(\kappa k^2+\alpha)\right\}K_{sk}-\left\{(\beta+\alpha)\frac{d}{dt}+(\kappa+\alpha)\right\}kG_{ck}=0
\end{aligned}\right\} \tag{8}$$

The notation α is defined as

$$\alpha=\frac{\kappa^2-\beta^2}{2(1+\nu)}.$$

By solving Eqs.(7), general solutions of $G_0(t)$ and $K_0(t)$ are obtained as follows:

$$\left.\begin{aligned}
G_0(t)&=C_{G01}e^t+C_{G02}e^{-t}\\
K_0(t)&=C_{K01}e^t+C_{K02}e^{-t}
\end{aligned}\right\}, \tag{9}$$

where $C_{G01}, C_{G02}, C_{K01}$ and C_{K02} are constants calculated from boundary conditions. Eq.(8) is rather complex to be solved. Primarily, four eigen values of Eqs.(8) are calculated as

$$\lambda_{k1}\sim\lambda_{k4}=\ k+1,\ -k-1,\ k-1,\ -k+1. \tag{10}$$

Considering $\lambda_{13}=\lambda_{14}=0$ for $k=1$, the general solutions of $G_{c1}(t), G_{s1}(t), K_{c1}(t), K_{s1}(t)$ of the forms are obtained.

$$\left.\begin{aligned}
G_{c1}(t)&=\sum_{j=1}^{2}A_{1j}\exp(\lambda_{1j}t)+A_{13}+A_{14}t\\
G_{s1}(t)&=\sum_{j=1}^{2}B_{1j}\exp(\lambda_{1j}t)+B_{13}+B_{14}t\\
K_{c1}(t)&=\sum_{j=1}^{2}\eta_{1j}B_{1j}\exp(\lambda_{1j}t)+(B_{13}+\eta_{13}B_{14})+B_{14}t\\
K_{s1}(t)&=-\sum_{j=1}^{2}\eta_{1j}A_{1j}\exp(\lambda_{1j}t)-(A_{13}+\eta_{13}A_{14})-A_{14}t
\end{aligned}\right\} \tag{11}$$

where

$$\eta_{11} = -\frac{5-4\nu}{-1+4\nu}, \quad \eta_{12} = 1, \quad \eta_{13} = \frac{1}{3-4\nu} \tag{12}$$

And general solutions of $G_{ck}(t), G_{sk}(t), K_{ck}(t)$ and $K_{sk}(t)$ for $k = 2,3,\ldots$ are derived as follows:

$$\left.\begin{aligned} G_{ck}(t) &= \sum_{j=1}^{4} A_{kj} \exp(\lambda_{kj} t) \\ G_{sk}(t) &= \sum_{j=1}^{4} B_{kj} \exp(\lambda_{kj} t) \\ K_{ck}(t) &= \sum_{j=1}^{4} \eta_{kj} B_{kj} \exp(\lambda_{kj} t) \\ K_{sk}(t) &= -\sum_{j=1}^{4} \eta_{kj} A_{kj} \exp(\lambda_{kj} t) \end{aligned}\right\} \tag{13}$$

where

$$\left.\begin{aligned} \eta_{k1} &= -\frac{k+4(1-\nu)}{k-2(1-2\nu)}, \quad \eta_{k2} = 1 \\ \eta_{k3} &= -1, \qquad\qquad \eta_{k4} = \frac{k-4(1-\nu)}{k+2(1-2\nu)} \end{aligned}\right\} \tag{14}$$

And A_{kj} and B_{kj} $(k = 1,2,\ldots;\ j = 1 \sim 4)$ are also constants calculated from the boundary conditions.

Boundary Conditions at the Inner Radius

The boundary conditions at the inner radius of the rubber roller, R_{in}, are $u(R_{in},\theta) = v(R_{in},\theta) = 0$. Subsequently, the following equations are obtained

$$G_0(\ln R_{in}) = K_0(\ln R_{in}) = 0 \tag{15}$$

$$\left.\begin{aligned} G_{ck}(\ln R_{in}) = G_{sk}(\ln R_{in}) = 0 \\ K_{ck}(\ln R_{in}) = K_{sk}(\ln R_{in}) = 0 \end{aligned}\right\} \quad (k = 1,2,\cdots) \tag{16}$$

Boundary Conditions at the Outer Radius

The boundary conditions at the outer radius of the rubber roller, R_{out}, are expressed by two sets of Fourier series for two loading conditions.

First, for the normal unit force, the boundary conditions are :

$$\begin{aligned}\sigma_r(R_{out},\theta) &= \lim_{d\theta\to 0}\frac{1}{R_{out}d\theta}\\ &= \frac{1}{R_{out}}\delta(\theta)\\ &= \frac{1}{2\pi R_{out}}+\frac{1}{\pi R_{out}}\sum_{k=1}^{\infty}\cos k\theta \qquad (17)\\ \tau_{r\theta}(R_{out},\theta) &= 0 \qquad (18)\end{aligned}$$

where $\delta(\theta)$ is the Dirac's δ function.

Second, for the tangential unit force, the boundary conditions are :

$$\begin{aligned}\sigma_r(R_{out},\theta) &= 0 \qquad (19)\\ \tau_{r\theta}(R_{out},\theta) &= \frac{1}{2\pi R_{out}}+\frac{1}{\pi R_{out}}\sum_{k=1}^{\infty}\cos k\theta. \qquad (20)\end{aligned}$$

Solutions of the Green's Function

The boundary conditions at the outer radius, shown in Eqs.(17), (20), are expressed not by deformations but by stresses. However, these stresses are theoretically related to deformations.

$$\begin{aligned}\sigma_r &= \frac{E}{\kappa^2-\beta^2}\left\{\kappa\frac{\partial u}{\partial r}+\beta\left(\frac{u}{r}+\frac{1}{r}\frac{\partial v}{\partial\theta}\right)\right\} \qquad (21)\\ \tau_{r\theta} &= \frac{E}{2(1+\nu)}\left(\frac{1}{r}\frac{\partial u}{\partial\theta}+\frac{\partial v}{\partial r}-\frac{v}{r}\right) \qquad (22)\end{aligned}$$

By substituting Eqs.(5) and (6) to Eqs.(21) and (22) and considering the harmonic balance with the boundary conditions of Eqs.(17) and (18) or Eqs.(19) and (20), we obtain the equations of the Fourier coefficients in Eqs.(5) and (6). Ensuingly, it is finally determined that the Fourier coefficients by using the boundary conditions at the inner radius in Eqs.(15) and (16).

Contact Problem

In this section, the way to solve contact problem is shown.

Analytical Model and Assumption

Figure 3 depicts an analytical model of a flexible media transport mechanism consisted of a rubber-layered steel roller and a steel roller. The rubber is deformed by contact with the paper supported by the steel roller. Because Young's modulus of steel is larger than 10^5 times of that of rubber, the deformation of steel parts is ignored. $O-XZ$ is a Cartesian coordinate system whose origin is set on an undeformed surface of the rubber. The coordinates, $o-r\theta$, denote polar coordinates

whose origin is the center of the rubber roller. The rotation direction of each roller has been shown in the figure. Negative and positive X corresponds to the inlet and outlet of rotation, respectively.

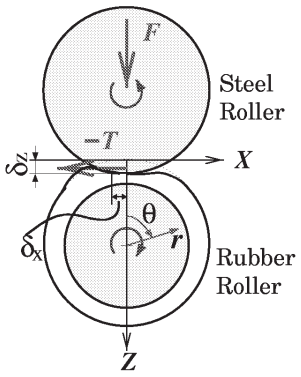

Figure 3: Contact model

In the previous section, Green's functions of the cylindrical rubber were derived analytically under the plane strain assumption. In this section, the following assumptions are further considered.

- Bending stiffness of the flexible media and deformations of the flexible media in the nip can be ignored.
- Tension T works on the flexible media directory and no break torque works on the steel roller.

In this section, contact normal and tangential pressure distributions, stick and slip area, strain of the rubber surface against the normal force F and the tension T are calculated. The rigid core of the rubber roller is fixed in space but rotatory. The steel roller can move along the Z-axis and the penetration depth is $\delta_Z(>0)$. The tension of the paper $-T$ is acting on the rubber surface so that a point on the free rubber surface at $X=0$ moves to $X=\delta_X<0$. The contact area is represented by angle, $-b\leq\theta\leq a$. In the inlet region, the rubber sticks to the steel surface and the constant strain ε_θ maintained along the θ-axis in the stick area because no slippage occurs in the stick area.

Deformation of the Rubber Surface due to Normal and Tangential Pressure

Assume that the point of application of force is θ and the point of observation of deformation is ψ, then $U_p(\psi)$ and $V_p(\psi)$ denote the normal and tangential deformation due to a normal pressure $p(\theta)$, respectively. Also, $U_q(\psi)$ and $V_q(\psi)$

denote the normal and tangential deformation due to a tangential pressure $q(\theta)$, respectively. These deformations are represented in the following equations using Green's functions.

$$U_p(\psi) = \int_{-b}^{a} u_p(R_{out}, \psi - \theta)\ p(\theta)\, R_{out}\, d\theta \tag{23}$$

$$V_p(\psi) = \int_{-b}^{a} v_p(R_{out}, \psi - \theta)\ p(\theta)\, R_{out}\, d\theta \tag{24}$$

$$U_q(\psi) = \int_{-b}^{a} u_q(R_{out}, \psi - \theta)\ q(\theta)\, R_{out}\, d\theta \tag{25}$$

$$V_q(\psi) = \int_{-b}^{a} v_q(R_{out}, \psi - \theta)\ q(\theta)\, R_{out}\, d\theta \tag{26}$$

We assume the linear elastic deformation in this analysis because the nonlinear deformation should not be utilized in the actual mechanism from the viewpoint of durability of the rubber roller.

Formulation of Contact Analysis

The condition equations of deformation, normal pressure, tangential pressure and boundary of the contact area, are shown in this subsection.

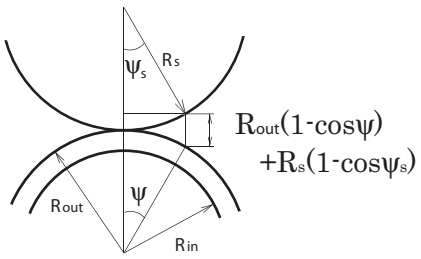

Figure 4: Initial gap

A steel roller whose outer radius is R_s is considered. The initial gap of the direction of Z is defined as shown in Fig.4. A deformation condition of the direction of Z was derived.

$$-\{U_p(\psi) + U_q(\psi)\}\cos\psi + \{V_p(\psi) + V_q(\psi)\}\sin\psi$$

$$= \delta_Z - R_{out}(1 - \cos\psi) - R_s(1 - \cos\psi_s) + \varepsilon_\theta R_{out}\,\psi\sin\psi, \tag{27}$$

where U_p, V_p, U_q, V_q are deformations on the rubber surface given by Eqs.(23)∼(26). And ψ_s is defined as the following equation.

$$\psi_s = \sin^{-1}\left\{\frac{R_{out}}{Rs}\sin\psi\right\} \tag{28}$$

A deformation condition of the direction of X should be considered in the stick area. Coulomb's frictional low, with a constant coefficient of friction, μ, and no difference between the adhesion and the sliding coefficient of friction between the paper and the rubber surface is assumed. The absolute value of the tangential pressure q doesn't exceed μp in the stick area and a deformation condition of the direction of X is given,

$$\begin{aligned}\{U_p(\psi)+U_q(\psi)\}\sin\psi+\{V_p(\psi)+V_q(\psi)\}\cos\psi \\ = \delta_X+\varepsilon_\theta R_{out}\,\psi\,\cos\psi.\end{aligned} \tag{29}$$

On the other hand, in the slip area, an alternative condition equation should be considered.

$$|q(\theta)| = \mu|p(\theta)| \tag{30}$$

From the equilibrium conditions of normal and tangential pressure, the normal and tangential loading forces are given by

$$F = \int_{-b}^{a}\{-p(\theta)\cos\theta+q(\theta)\sin\theta\}\,R_{out}\,d\theta, \tag{31}$$

$$T = \int_{-b}^{a}\{p(\theta)\sin\theta+q(\theta)\cos\theta\}\,R_{out}\,d\theta. \tag{32}$$

Boundary conditions of the contact area are given as follows.

$$p(-b) = p(a) = 0\ ,\ q(-b) = q(a) = 0 \tag{33}$$

In the calculation procedure, normal and tangential pressures, p and q, are defined on 50 points in the contact area and p, q, δ_Z, δ_X, ε_θ, a and b are iteratively calculated by using Eqs.(27), (33).

Calculated Result

Calculated results of the relation of load force and penetration depth are mainly discussed below.

The examples of the relation of load force and penetration depth obtained by theoretical analysis are shown in Fig.5. In the calculation, the outer radius of each roller is 15mm, Young's Modulus of rubber are 5.57MPa and 1.35MPa, Poisson's

ratio of rubber ν is 0.49, friction coefficients μ is 0.5 and the normal loading force F is changed from 100 to 700N/m. In all calculation, tangential loading force T is 0. In this calculation, Young's Modulus of rubber E_r, rubber thickness T_r, load force F were chosen as variable parameters.

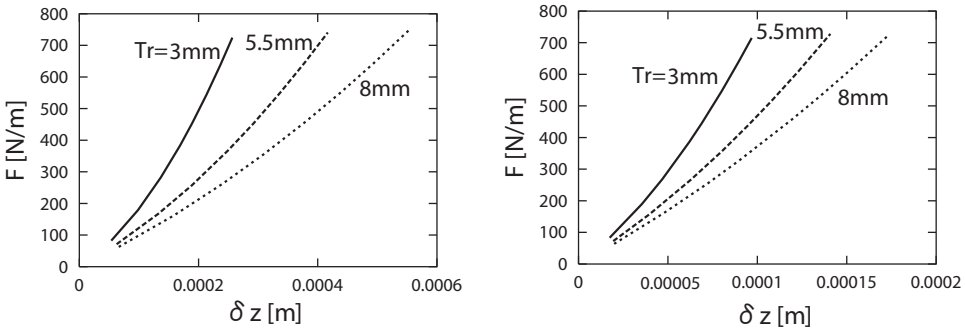

(a) 30Hs (b) 70Hs

Figure 5: Nonlinear spring characteristics of rubber roller

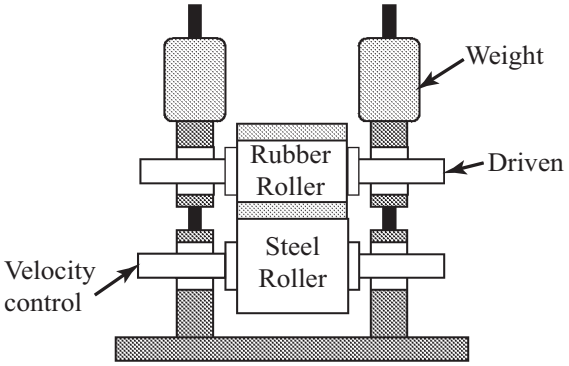

Figure 6: Experimental setup of short roller

It is found from Fig.5 that the thinner the rubber is the harder the rubber roller behaves. And, each plot can well approximate with quadratic function that throughs origin. For example, the case of $T_r = 5.5$mm, $E_r = 5.57$MPa, approximate quadratic function is

$$F = 3.424 \times 10^6 \delta_z + 1.253 \times 10^{10} \delta_z^2.$$

Preliminary Experiment and Discussion

Experimental Apparatus and Conditions

In order to confirm the validity of our calculated results, an experimental setup shown in Fig.6 was prepared. The radius and length of each roller is 15mm and 40mm, respectively. The bearing span of rollers is 55mm. The steel roller is a drive roller that is actuated by a motor with a velocity controller. The rubber roller is a driven roller that rotates freely and is supported in a vertical plane with guide shafts. The normal loading force is given to the rollers by weights and decides the penetration depth. In order to obtain the relation of load force and penetration depth, the normal loading force F was changed from 100 to 700N/m. The penetration depth was measured as the displacement of rubber roller unit by a CCD camera and monitor. All experiments were performed with rotational speed of the steel roller of 10rpm.

Six silicon rubber rollers are prepared for experiments. The thickness of rubbers are 3.0mm,5.5mm and 8.0mm. The hardness of the rubbers are s =70 Hs and s =30 Hs and the value of Young's Modulus was calculated from the hardness with Gent's equation[14].

$$E(\mathrm{MPa}) = 9.8 \times 10^{-2} \frac{s+7.31}{0.0456(100-s)} \tag{34}$$

Comparison Between Calculated and Experimental Results

Figure 7 indicates the relation of load force and penetration depth obtained experimentally. Eight experiments were achieved for one loading condition and the maximum, average and minimum values are shown in the figures. It is noted that the calculation results agree well with experimental ones.

Analysis of the Longitudinal Distribution of the Nip Pressure

Long rollers whose shaft deflection cannot be ignored have the longitudinal distribution of the nip pressure as shown in Fig.8. In this case, the rubber deformation is three-dimentional but it can be modeled with two-dimensional contact mentioned before because the out-of-plane strain is much smaller than the plane strain. In this section, an analytical method that is based on the results of the two-dimensional contact analysis and can estimate the longitudinal distribution of nip pressure of the long rollers is developed.

Two-dimensional model of rubber deformation leads a simple model with parallel independent nonlinear springs shown in Fig.9. The nonlinear characteristics of springs were obtained in the two-demensional analysis shown in Section . The static deformation of the rubber roller shaft $z_r(y)$ should be considered in the analysis of the longitudinal distribution of the nip pressure. When the longitudinal distribution of the nip pressure $F(y)$ is given, $z_r(y)$ is calculated from the following

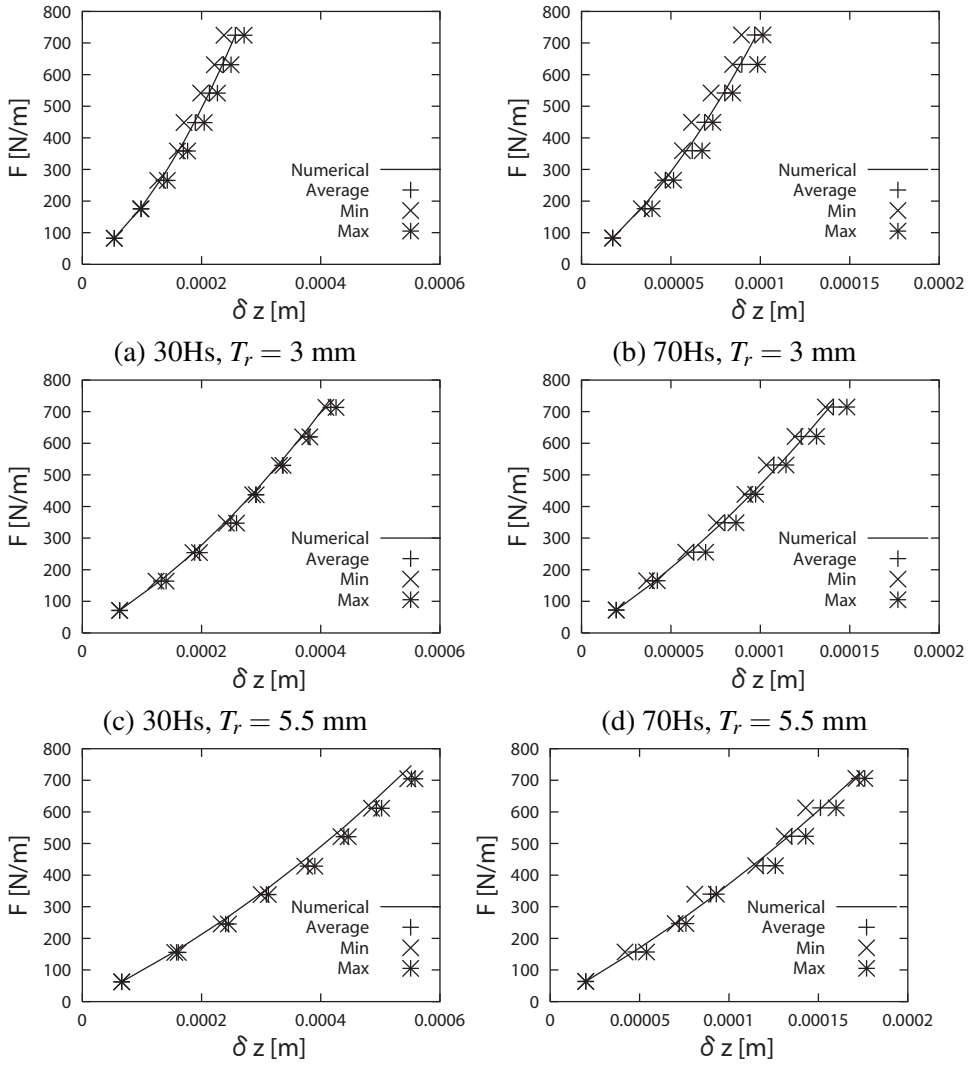

(a) 30Hs, $T_r = 3$ mm (b) 70Hs, $T_r = 3$ mm

(c) 30Hs, $T_r = 5.5$ mm (d) 70Hs, $T_r = 5.5$ mm

(e) 30Hs, $T_r = 8$ mm (f) 70Hs, $T_r = 8$ mm

Figure 7: Experimental results of relation of load force and penetration depth

equation.

$$E_s I_s \frac{d^4 z_r(y)}{dy^4} = F(y), \tag{35}$$

where E_s and $I_s = (\pi R_c^4)/4$ are an elastic modulas and the second moment of area of the rubber roller shaft, respectivelly.

On the other hand, the static defromation of the steel roller was ignored in the analysis, because it is thicker than the rubber roller shaft. In the calculation

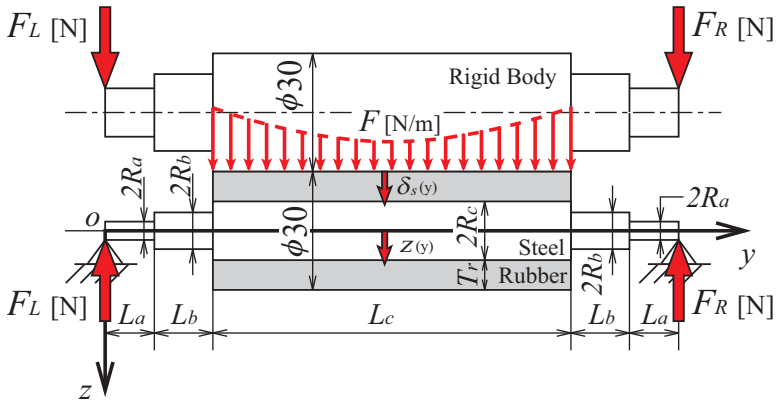

Figure 8: Calculation model

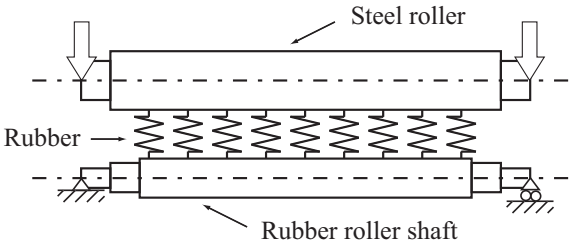

Figure 9: Nonlinear spring model

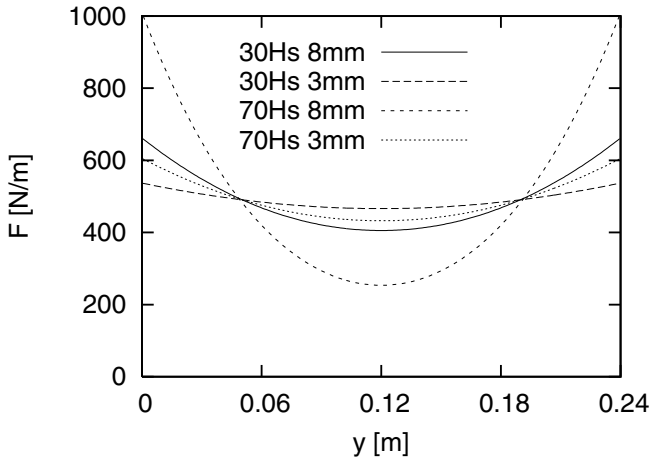

Figure 10: Longitudinal distribution of nip pressure

procedure, the stiffness of the rubber roller shaft can be calculated from Eq.(35) by FEM and utilized with nonlinear stiffness of rubber.

Examples of calculated longitudinal distribution of the nip pressure of straight rollers were shown in Fig.10. Load force acting on each side was assumed to be 58.8N in these calculations. More than 10% deviation of the longitudinal distribution of the nip pressure is observed even in the bast case of the examples.

Crown Design

In this section, the way to uniform the longitudinal distribution of nip pressure using crown roller is shown.

A crown roller generally means a steel roller with crown shape in its diameter. However, other types of crown rollers, i.e. a rubber roller with crown shape in its inner or outer diameter were able to assumed. Because it is difficult to fabricate rubber with high accuracy, a rubber roller with crown shape in its outer diameter was ignored. Thus, two types of crown roller were discussed. The dimensions of each type of crown roller were calculated with a computer program whose flow chart is shown in Fig.11.

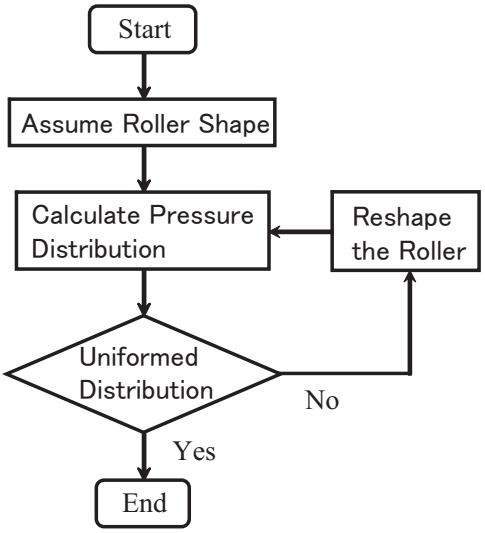

Figure 11: Flow chart of crown calculation

Crown of Steel Roller

In this subsection, design procedure of crowned steel roller is shown.

From the two-dimensional analysis, nonlinear spring characteristics of the rubber roller is derived as

$$F(y) = b_1 \delta_z(y) + b_2 \delta_z(y)^2 \tag{36}$$

Notations b_1 and b_2 were resulting coefficients derived from nonlinear spring characteristics of the rubber roller. From this equation, the following equation is obtained.

$$\delta_z(y) = \frac{-b_1 + \sqrt{b_1^2 + 4b_2 F(y)}}{2b_2} \tag{37}$$

In the case of straight rollers, each position of the rubber surface should move a constant distance by contact. The rubber roller shaft deflection is a function of y, then the penetration depth of rubber roller should be a function of y. This is the reason of the nonuniform longitudinal distribution of nip pressure. In order to obtain uniform longitudinal distribution of nip pressure, constant penetration depth of rubber roller required. In the design procedure, a reference penetration depth is chosen and the diameter of the steel roller at y, $R_s(y)$, is changed iteratively so that the penetration depth at y coincides with that of the reference point y_r.

$$R_s(y)_{new} = R_s(y)_{old} - \delta_z(y) + \delta_z(y_r) \tag{38}$$

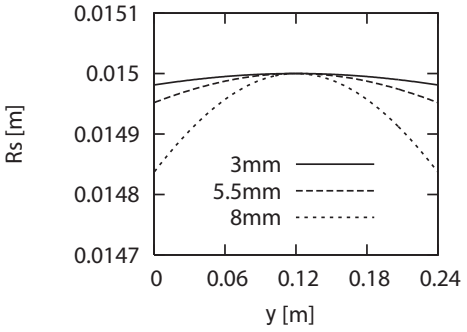

Figure 12: Example of crown shape of steel roller

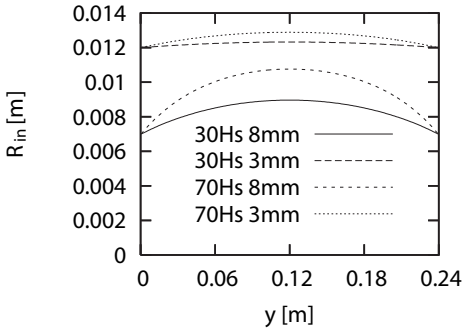

Figure 13: Example of crown shape of rubber roller shaft

Figure 12 shows an example of crown shape derived from calculation. The crown shape actually agrees with the rubber roller shaft deflection loaded static uniform load force. It is found from Fig.12, calculated crown height $R_{smax} - R_{smin}$ is less than $20\mu m$. Thus, it can be concluded that uniform longitudinal distribution of nip pressure is hardly achieved practically with the crowned steel roller.

Crown of Rubber Roller

In this subsection, design procedure of crowned rubber roller shaft is shown.

Thinner rubber has harder spring characteristics. Using this property, longitudinal distribution of nip pressure could be uniformed. Thus, the rubber should be thickened where load force is strong, or be thinned where load force is weak.

As mentioned before, the rubber roller has nonlinear spring characteristics shown in Eq.(36). And the coefficients of b_1 and b_2 in this equation are functions of the inner radius of the rubber roller. These coefficients were obtained for various inner radius by two-dimensional analysis and derived interpolation functions of them.

$$b_k(r) = \sum_{j=1}^{B+1} C_{kj} R_{in}^{j-1} \qquad (k = 1,2), \tag{39}$$

where R_{in} is a radius of the rubber roller shaft and B is the number of calculated case. Thus,

$$\begin{aligned} F(y) &= b_1(y)\delta_z(y) + b_2(y)\delta_z(y)^2 \\ &= \sum_{j=1}^{B+1} \delta_z(y) \left\{ C_{1j} + \delta_z(y) C_{2j} \right\} R_{in}(y)^{j-1} \end{aligned} \tag{40}$$

From this equation, the radius of the rubber roller shaft at y that gives the same nip pressure with that of the reference point y_r was callculated iterativelly by the following equation.

$$R_{in}(y)_{new} = \frac{F(y_r) - F(y)}{F'(y)} + R_{in}(y)_{old} \tag{41}$$

where

$$F'(y) = \sum_{j=1}^{B+1} (j-1)\, \delta_z(y) \left\{ C_{1j} + \delta_z(y) C_{2j} \right\} R_{in}(y)_{old}^{j-2}$$

Examples of crown shape of the rubber roller shaft are shown in Fig.13. In these cases, the roller end was chosen as the reference position. Even in the case of soft and thin rubber, the calculated crown height $R_{inmax} - R_{inmin}$ is about $300\mu m$. It can be concluded that uniform longitudinal distribution of nip pressure will be achieved practically with the crowned rubber roller shaft.

Experiment and Discussion

In this section, the experiment of crowned rubber roller shaft is shown.

Experimental Apparatus and Conditions

Only one type crown rollers were fabricated that were rubber rollers with crown shape in its internal diameter. One of crown rollers proparties are 70Hs hardness rubber, the thickness of rubber is 3mm at the edge of roller. Those of the other one are 30Hs hardness rubber, the thickness of rubber is 3mm at the edge of roller. These rollers were designed for 58.8N loading force for each side of rollers.

In order to confirm the validity of our calculated results, an experimental setup shown in Fig.14 was prepared. To measure the longitudinal distribution of nip

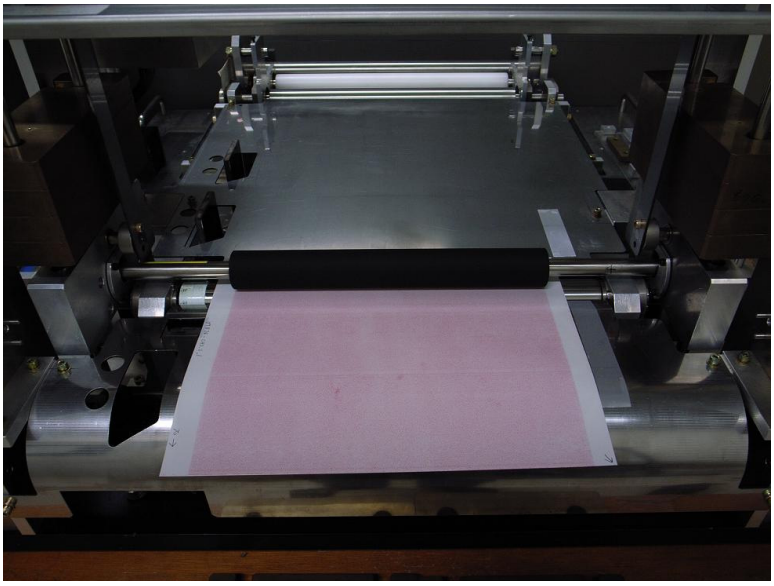

Figure 14: Test bench of Crown roller

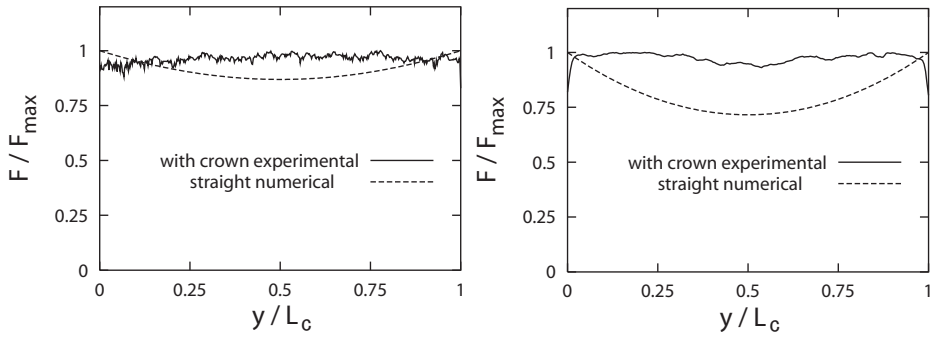

(a) 30Hs (b) 70Hs

Figure 15: Experimental result of longitudinal distribution of nip pressure of crown roller

pressure, pressure measuring film called PRESCALE was used. The loading force is 58.8N for each side of rollers. Crown roller is drived by servo motor of 10rpm. Straight steel roller rotates freely.

Comparison Between Calculated and Experimental Results

Because of PRESCALE characteristics, measured pressure is very noisy. So the average of pressure of its driving direction is derived from measured data. And PRESCALE can't measure precise puressure, the averaged pressure was normal-

ized with its maximum value. The result of these calculation of experimental data is called normalized pressure distribution. If longitudinal distribution of nip pressure is uniformed, normalized pressure distribution is flat and its value is 1.

Figure 15 shows examples of the experimental results. Compared to the calculation results of normalized pressure distribution of straignt rollers, our crown roller gives well uniformed pressure distribution.

Table 1: Roller demensions

	a	b	c
L[mm]	7	93	240
R[mm]	5	7	9.5

Conclusion

In this paper, firstly, two-dimensional contact problem was solved theoretically with Green's functions of a rubber roller with a rigid core. And the relation of load force and penetration depth was obtained experimentally and theoretical results were confirmed by experimental results.

Secondly, the way to obtain crown shape that can uniform longitudinal dostribution of nip pressure was shown. In this design procedure, the results of two-dimensional contact problem was utilized. Experimental results were also compared with theoretical ones and discussed.

The results of this study are summarized as follows:

1. The way to obtain Green's function was shown.
2. The way to solve two-dimentional contact problem was shown.
3. Calculated results were confirmed with experiments of the relation of load force and penetration depth.
4. The method to obtain the londitudinal pressure distribution of nip pressure of a long rollers was revailed.
5. The dedign procedure to obtain crown shape based on the calculated relation of load force and penetration depth was shown.
6. Designed crown rollers were fabricated and the performances of them were confirmed with experiment.

References

1. Fujimura, H., and Ono, K., 1996, "Analysis of paper motion driven by skew-roll paper feedinf system," *Transactions of JSME*, Vol.62(C), No.596, pp.1354-1360.(in Japanese)

2. Hertz, H., 1881, "Über die Berührung fester elastischer Koerper," *J. Reine Angew. Math.*, No.92, pp.156-171.
3. Hannah, M., 1951, "Contact Stress and Deformation in a thin Elastic Layer," *Quart. Journ. Mech. And Applied Math.*, Vol.4, Pt.1, pp.94-105.
4. Parish, G.J., 1958, "Measurements of pressure distribution between metal and rubber covered rollers," *British Journal of Applied Physics*, Vol.9, pp.158-161.
5. Bentall, R.H., and Johnson, K.L., 1967, "Slip in the Rolling Contact of Two Dissimilar Elastic Rollers," *International Journal of Mechanical Sciences*, Vol.9, pp.389-404.
6. Hahn, H.T., and Levinson, M., 1974, "Indentation of an Elastic Layer(s) Bonded to a rigid Cylinder - I. Quasistatic Case without Friction," *International Journal of Mechanical Sciences*, Vol.16, pp.485-502.
7. Gupta, P.K., and Walowit, J.A., 1974, "Contact Stresses Between an Elastic Cylinder and a Layered Elastic Solid," *Transactions of the ASME*, Series F, Vol.97, No.2, pp.250-257.
8. Soong, T.C., and Li, C., 1981, "The steady rolling contact of two elastic Layer bonded cylinders with a sheet in the nip," *International Journal of Mechanical Science*, Vol.23, pp.263-273.
9. Soong, T.C., and Li, C., 1981, "The rolling contact of two elastic-Layer-covered Cylinders driving a loaded sheet in the nip," *Transaction of the ASME, Jounal of Applied Mechanics*, Vol.48, pp.889-894.
10. Kalker, J.J., 1991, "Viscoelastic Multilayered Cylinders Rolling with Dry Friction," *Transaction of the ASME, Journal of Applied Mechanics*, Vol.58, No.3, pp.666-678.
11. Wu, J., Nakazawa, M., Kawamura, T.,Baba, H., Kamimura, H., Tanaka, N., and Miyahara, K., 1999, "Study on Elastic Deformation Properties of the Blanket in Offset Printing," *JSME International Journal*, Series A, Vol.42, No.3, pp.388-393.
12. Okamoto, N., Ohtani, K., Misawa, K., Yoshida, K., 2001, "Study on Velocity Characteristics and Mechanics of Paper Feeding with Rubber-Covered Roller Drive," *Transaction of the JSME*, Vol.67(C), No.654, pp.475-482. (in Japanese)
13. Johnson, K.L., 1985, *Contact Mechanics*, Cambridge University press
14. A.N.Gent, 1958, "On the relation between indentation hardness and Young's modulus," *Transactions of the Institution of the Rubber Industry*,34